

# Analysis and Design of an Optimum Novel Millimeter T and Y-Junction SIW Power Dividers Using the Quick Finite Element Method

<sup>1</sup>FELLAH BENZERGA, <sup>1</sup>MEHADJI ABRI, <sup>2</sup>HADJIRA ABRI BADAOUY and <sup>3</sup>JUNWU TAO

<sup>1</sup>LTT Laboratory,

Faculty of Technology, University of Tlemcen, ANI GTK

<sup>1</sup>STIC Laboratory,

Faculty of Technology, University of Tlemcen, ANI GTK

<sup>3</sup>LAPLACE - LPLACE

INPT-ENSEEIH, 2 rue Charles Camichel, BP 7122

31071 Toulouse, Cedex 7, FRANCE

fellahtl@yahoo.fr, abrim2002@yahoo.fr, elnbh@yahoo.fr, tao@laplace.univ-tlse.fr

*Abstract:* - The aim of this paper is to present a novel technique for the design of millimetre substrate integrated waveguide (SIW) power dividers based on the Quick Finite Element Method. The return losses, transmission coefficients and the field's distribution are presented and analyzed by this technique. To present the validity and the performances of our structures, the obtained results are compared with CST commercial software in the band frequencies from 40 to 75 GHz. The numerical simulation program can provides useful design information as well as physical insights for frequencies in the millimeter wave range.

*Key-Words:* - T and Y junction power dividers, two dimension Finite Element Method 2D-FEM, QFEM, substrate integrated waveguide SIW, millimeter band.

## 1 Introduction

The substrate integrated waveguide power dividers are building blocks of many microwave and millimeter-wave integrated circuits and systems. Such as filters [1-2], couplers and antenna feeders are just a few applications [3-4]. The first substrate integrated waveguide (SIW) was proposed by Deslandes and Wu in 2001 [5]. In recent years, many devices have been developed using SIWs: transitions to different planar lines [6-7], mixers and oscillators [8-9], etc. Due to the advantages of this technology, such as low cost, high Q-factor, low insertion loss, easy to be integrated and high density layout, SIWs are a good compromise between the performance of classical waveguides and planar circuits in terms of quality factor and losses. The SIW is synthesized on the substrate with linear arrays of metalized via holes, but metalized grooves could also be used [10]. Since all the components are designed on the same substrate, a planar fabrication technique can guarantee excellent mechanical tolerances as well as tuning-free design [11].

The structures of SIW power dividers are analyzed by finite element method; the advantages of the FEM are that can analyze very complex geometry, a wide variety of engineering and electromagnetic problems [12].

In this paper, an attempt was made to apply the two dimensional finite element method in H-plane case to determine return losses, insertion losses and field distributions of optimized T and Y junction SIW power dividers operating in the range frequencies from 40 to 75 GHz for millimeter wave applications. In order to test the performances of the proposed approach, the obtained results by the 2D-FEM are compared with those obtained using the CST microwave studio commercial software.

In this paper, the numerical method is used to analyze the SIW power dividers mode features. The method is a two dimension finite element method (2D-FEM) algorithm written under Matlab environment (QFEM) for the modeling of power dividers properties.

The work of this paper is organized as follows: the SIW finite element theory applied for waveguide junction problem using the weak form of the Helmholtz equation is developed in section 2. The SIW power dividers design procedure is given in section 3. Simulation results in terms of return loss, transmission coefficients and electromagnetic fields distribution are exposed in section 4. Finally, the conclusion is given in section 5.

## 2 The Finite Element Formulation

A waveguide discontinuity power divider is a particular case in which the ports are waveguides. Let us consider a structure that is excited through the fundamental mode TE<sub>10</sub> at a given port. However, at the discontinuity the complex formulas have been determined by the finite element method procedure. The FEM is applied in the region Ω and is fortified by a perfectly conducting wall Γ<sub>0</sub> as shown in Fig. 1. The electric and magnetic field can be calculated by the FEM formulation [9] in inhomogeneous region Ω. The scalar electric field E<sub>y</sub> satisfies the Helmholtz equation such as :

$$\nabla_t \left( \frac{1}{\mu_r} \nabla_t E_y \right) + k_0^2 \epsilon_r E_y = 0 \quad (1)$$

Where: μ<sub>r</sub> and ε<sub>r</sub> are the permeability and permittivity, respectively, of the material in the waveguide. The homogeneous Dirichlet boundary condition for the port *k* is:

$$E_y = 0, k=1, \dots, j \quad (2)$$

At the metallic wall Γ<sub>0</sub> of the waveguide junction and the appropriate continuity conditions for the electric and magnetic fields at each port:

$$E_y|_{\Gamma_k} = E^k_{y_{siw}}, \quad k = 1, \dots, j \quad (3)$$

$$H_x|_{\Gamma_k} = H^k_{x_{siw}}, \quad k = 1, \dots, j \quad (4)$$

The electric field at each port:

$$\frac{\partial E_y}{\partial n} \Big|_{\Gamma_k} = \frac{\partial E^k_{y_{siw}}}{\partial z}, \quad k = 1, \dots, j \quad (5)$$

The variational formulation is obtained by multiplying the Helmholtz equation (1) with a weighting function *w*. Integration by parts (Green's identity) is applied to the double curl term and a boundary condition term [12] appears in the variational formulation:

$$\iint_{\Omega} w \nabla_t \cdot \left( \frac{1}{\mu} \nabla_t E_y \right) d\Omega - k_0^2 \iint_{\Omega} \epsilon_r w E_y d\Omega - \int_{\Gamma_k} w \frac{\partial E^k_{y_{siw}}}{\partial z} d\Gamma_k = 0 \quad (6)$$

In the fig. 1, the region Ω is divided into Ne finite elements and in each of them the approximation

$\bar{E}_y^{(e)}$  of the exact solution is expressed via a grouping of nodal basis functions such as :

$$\bar{E}_y^{(e)}(x, y) = \sum_{j=1}^{N^{(e)}} \bar{E}_{y_j}^{(e)} \alpha_j^{(e)}(x, y) \quad (7)$$

Where: α<sub>*j*</sub><sup>(*e*)</sup>(*x*,*y*) and  $\bar{E}_{y_j}^{(e)}$  (*j* = 1...N<sup>(*e*)</sup>) are the interpolating nodal shape functions defined on element (*e*) and the values of the total field, respectively. The weighting functions W<sub>*i*</sub><sup>(*e*)</sup> are defined by the shape functions, W<sub>*i*</sub><sup>(*e*)</sup> = α<sub>*i*</sub><sup>(*e*)</sup> (*i* = 1. . N<sup>(*e*)</sup>).

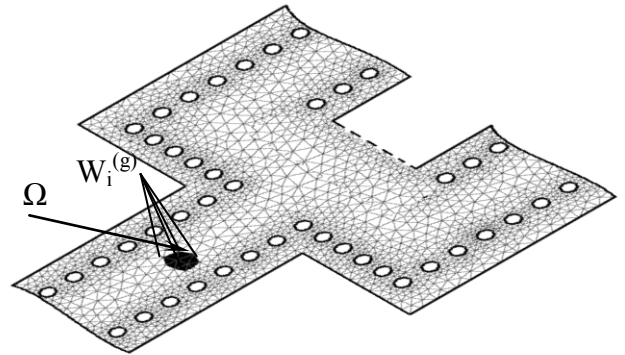


Fig. 1 Weighting functions W<sub>*i*</sub><sup>(g)</sup> centered at the same global node *i*.

The solution of (8) in the case of H-plane using finite elements, the finite element analysis of any problem micro wave.

R<sub>*i*</sub><sup>(*e*)</sup> is the residue relative to the *i*<sup>th</sup> weighting function, with:

$$\frac{1}{\mu_r} \iint_{\Delta^{(e)}} \nabla_t \alpha_i^{(e)} \cdot \nabla_t \bar{E}_y^{(e)} d\Omega - k_0^2 \epsilon_r \iint_{\Delta^{(e)}} \alpha_i^{(e)} \bar{E}_y^{(e)} d\Omega - \sum_{k=1}^N \int_{\Gamma_k^{(e)}} \alpha_i^{(e)} \frac{\partial E_{y_{siw}}^{(k)}}{\partial z^{(k)}} d\Gamma_k = 0 \quad (8)$$

Alternatively, in matrix form:

$$\frac{1}{\mu_r} [S^{(e)}] \cdot [\bar{E}_y^{(e)}] - k_0^2 \epsilon_r [T^{(e)}] \cdot [\bar{E}_y^{(e)}] + \sum_{k=1}^N \left\{ [C_k^{(e)}] \cdot [B_k] - [H_k^{(e)}] \right\} = [R^{(e)}] \quad (9)$$

The matrices [S<sup>(*e*)</sup>] and [T<sup>(*e*)</sup>] present the scalar nodal element,  $[\bar{E}_y^{(e)}]$  is the vector of nodal, [B<sub>*k*</sub>] is a column vector and  $[C_k^{(e)}], [H_k^{(e)}]$  come from the contour integrals at the *k* = 1...N ports [10].

In (10) present the matrix [F] assembles the two matrices [S<sup>(e)</sup>] and [T<sup>(e)</sup>] with a dimension of (N<sub>n</sub> × N<sub>n</sub>), with N<sub>n</sub>total number of nodes, [C] assembles the matrix [C<sub>k</sub><sup>(e)</sup>] and the vector [H<sub>k</sub><sup>(e)</sup>] with a dimension of (N<sub>n</sub> × (N × M)) and [H<sup>inc</sup>] presented by the column (N × 1), is given by:

$$[F]. [\bar{E}] + [C]. [B] = [H^{inc}] \quad (10)$$

Where:

[B] is column vector with dimension((N × M) × 1). In this matrix, the unknowns are the column vectors  $\bar{E}$  and [B].

The matrix  $\bar{E}$  contains the coefficients of the finite element approximation of the electric field, [B] stores the amplitude of the transmitted field at the ports, then the only nonzero entry of vector [H<sup>inc</sup>].

The global system of equations to be solved and can be assembled into a block matrix equation similar to that built in the case of waveguide discontinuity characterization:

$$\begin{bmatrix} [A] & [D] \\ [C] & [F] \end{bmatrix} \cdot \begin{bmatrix} [B] \\ [E] \end{bmatrix} = \begin{bmatrix} [E^{inc}] \\ [H^{inc}] \end{bmatrix} \quad (11)$$

Where: [F] the sparse and symmetric finite element matrix .Which is can be solved using the same structure as that in (11), even though with a doubled number of unknowns.

### 3 SIW power dividers design procedure

Let us present in this section the SIW power dividers design procedure. The design formulas (12) of the SIW are given first by defining the width of the substrate. The distance between opposite via of the SIW is given by [10]:

$$W = w_{eff} + \frac{d^2}{0.95p} \quad (12)$$

The cut off frequency f<sub>c</sub> is defined by this formula:

$$f_c = \frac{c}{2\sqrt{\epsilon_r}} \left( W - \frac{d^2}{0.95p} \right)^{-1} \quad (13)$$

Where: d is the diameter metal pins, p is pitch (distance between the vias), c is the speed of light in vacuum, ε<sub>r</sub> the relative dielectric permittivity of the substrate and W the width spacing. The accuracy of this formula is valid for:

$$p < \frac{\lambda_0}{2\sqrt{\epsilon_r}} \quad (14)$$

$$p \leq 2d \quad (15)$$

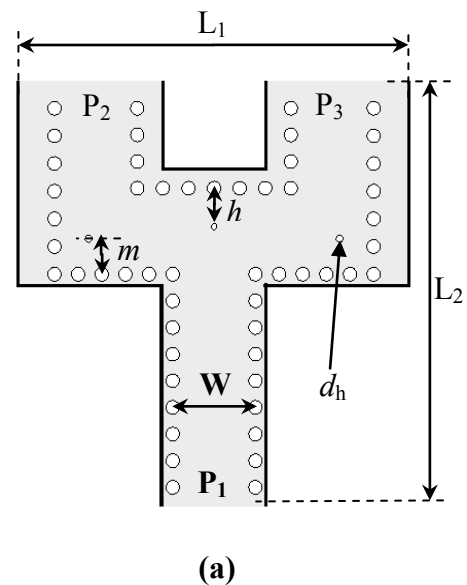
Where: λ<sub>0</sub> is the wavelength in free space.

### 4 Simulation results

To validate the numerical method approach, let us present in this section the simulation results of an H-plane discontinuity T and Y junction SIW power dividers operating in millimeter applications frequency range from 40 to 75 GHz.

The SIW structures are excited using TE<sub>10</sub> fundamental mode. For implementation, Arlon Cu 217LX low loss with material was used for both layers, with dielectric substrate of ε<sub>r</sub> = 2.2 and tanδ = 0.0009, and a substrate thickness of about 0.508 mm. Let us present respectively in Fig. 2 and 4 the optimized T and Y-junction SIW group power dividers. Note that the simulations were achieved using an Apple i7 CPU M 620, with 8 Go RAM memory on the same computer.

Fig. 2 (b) and Fig. 4 (b) show the tetrahedral mesh obtained after applying the Delaunay algorithm, the Delaunay refinement are effective both in theory and in practice[13]. Delaunay refinement algorithms operate by maintaining a Delaunay or constrained Delaunay triangulation, which is refined by inserting carefully placed vertices until the mesh meets constraints on triangle quality and size . Let us present the mesh for each structure in the Fig. 2 (b) and Fig. 4 (b).



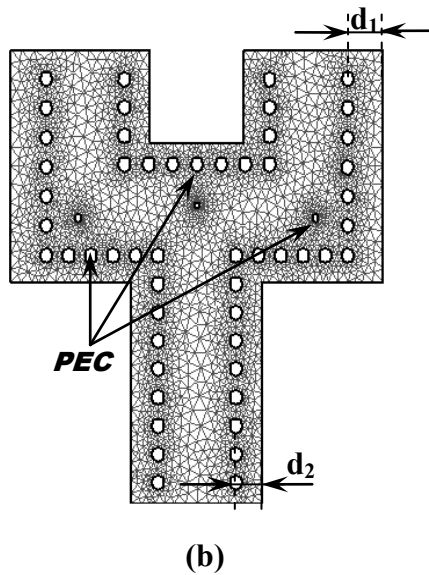
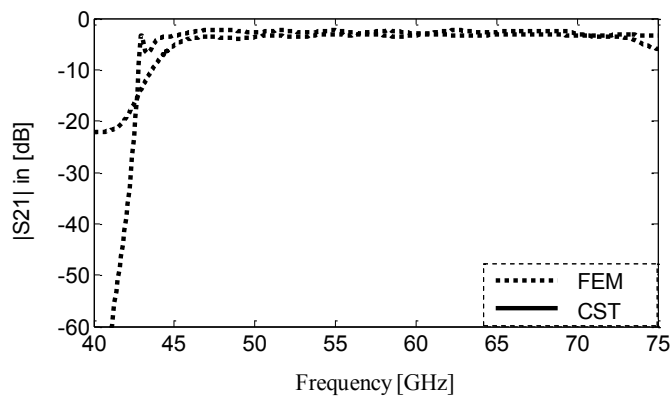
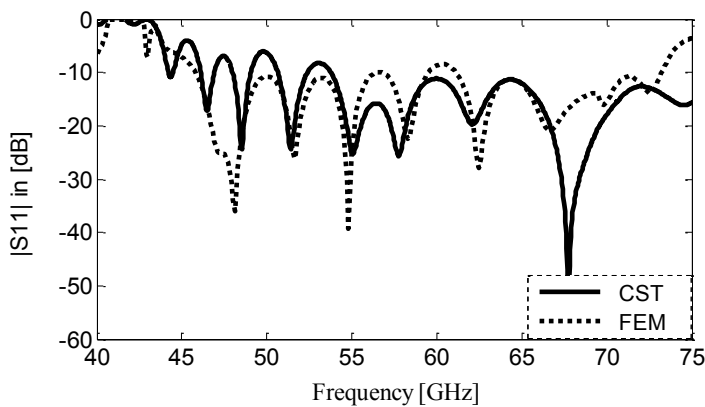


Fig. 2 (a). Optimized T-junction with inductive post power divider structure . (b) The generated mesh by FEM. The parameters are set as:  $w= 2.60\text{mm}$ ,  $d=0.40\text{ mm}$ ,  $p=0.70\text{ mm}$ ,  $m=1.60\text{ mm}$ ,  $h=1.30\text{ mm}$ ,  $d_h=0.20\text{ mm}$ ,  $d_1=0.70\text{ mm}$ ,  $d_2=0.70\text{ mm}$ ,  $L_1=10.35\text{ mm}$  and  $L_2= 9.50\text{ mm}$ .



(b)

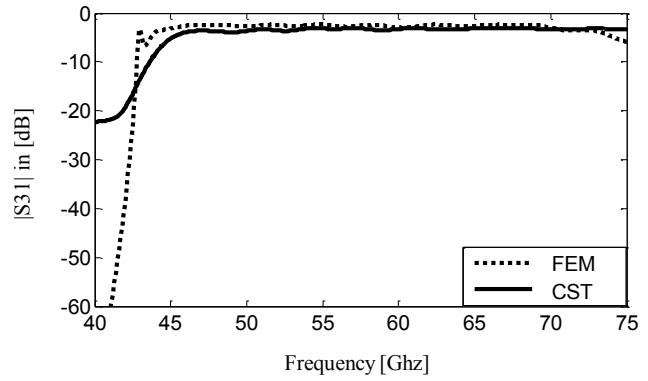


Fig. 3 Comparison between the finite element method and CST Microwave studio software results for SIW T-junction power dividers. (a) Return loss. (b)  $S_{21}$  Insertion loss. (c)  $S_{31}$  Insertion loss.

The optimize values of diameter of the post  $d_h=0.2\text{ mm}$  and its location  $h=1.2\text{ mm}$ , the ratio of the reflection power to the incident power at port 1 is indicted in the Fig. 2, The minimum reflection is obtained for values  $h$  and  $d_1$ .

This comparison between the CST and the Finite Element Method results for respectively the return loss and insertion losses for port 2 and 3 are indicated in Fig. 3. As shown in Fig. 3 (a), an excellent agreement is observed between the simulations results provided the FEM method and those of the CST Microwave studio software except for some frequency range. It is noticed from Fig 3. (b) and (c) that the cut-off frequency is well predicted and showed with two methods. No transmission is possible for the frequency under this cut-off frequency witch is of about 42.5 GHz.

The Y-junction power divider with its geometric parameters is shown in Fig. 4. The designed Y-junction two-way power divider has the same width for both input SIW and output SIWs, which are designed to only support  $TE_{10}$  fundamental mode in the whole operating frequency range with a width of  $W$ . The input power must be equally divided into the two output SIWs by the metallic-vias in the middle. By optimizing the position  $L$ , good performances for the Y-junction two-way power divider can be obtained.

At the input port, the length  $L$  can greatly affect the average and width band frequency of the return loss. The initial goal with this structure was to obtain a lower return loss at cut-off frequency  $f_c = 50\text{ GHz}$ . After optimization using the CST software, the design curves are shown in Fig. 4 leads to an optimal length  $L=2.70\text{ mm}$ .

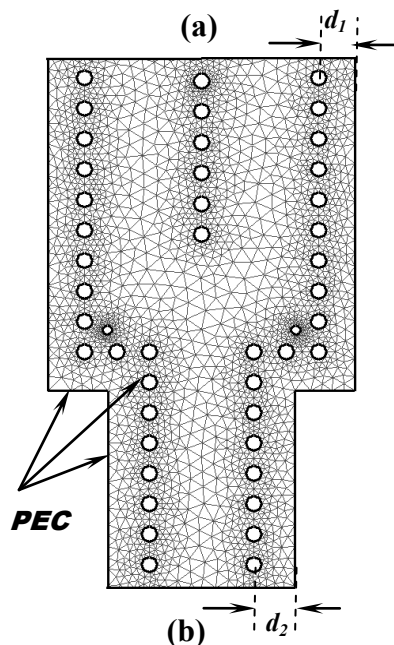
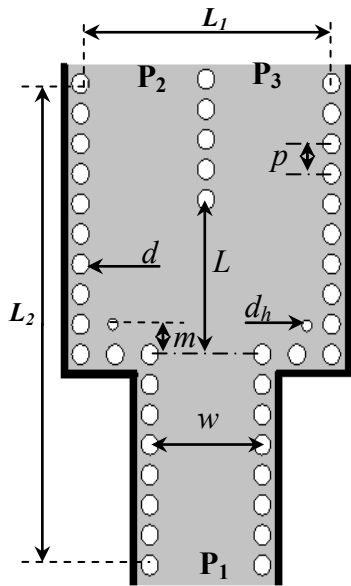
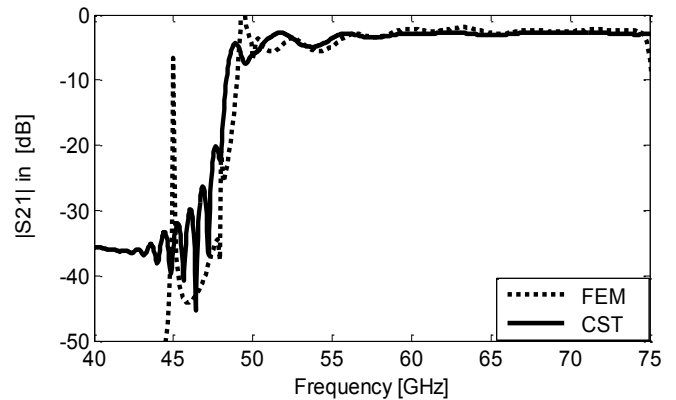
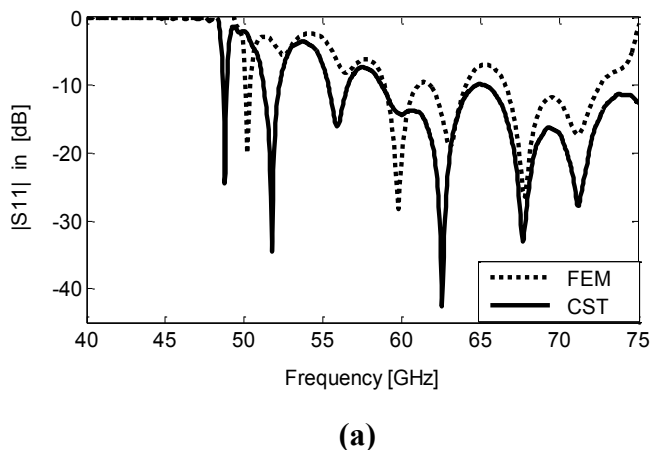
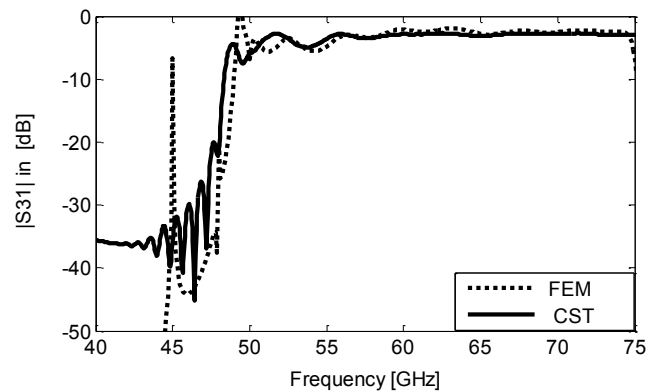


Fig. 4 Y-junction power divider,  $w = 2.5\text{mm}$ ,  $d = 0.40\text{mm}$ ,  $p = 0.70\text{mm}$ ,  $d_h = 0.20\text{mm}$ ,  $m = 0.50\text{mm}$ ,  $L = 2.70\text{mm}$ ,  $d_1 = 0.70\text{mm}$ ,  $d_2 = 0.70\text{mm}$ ,  $L_1 = 11.06\text{mm}$ ,  $L_2 = 5.30\text{mm}$ ,



(b)



(c)

Fig. 5 Comparison between the finite element method and CST Microwave studio software results for SIW Y-junction power dividers. (a) Return loss. (b)  $S_{21}$  Insertion loss. (c)  $S_{31}$  Insertion loss.

Fig. 5 depicts the simulations results of the return losses and the transmission coefficients obtained by the CST Microwave studio software and FEM method. As shown, there is a good agreement between the FEM and simulated results with CST. The computed return losses are less than -10 dB for the frequencies greater than 50 GHz, the corresponding transmission are almost identical between the FEM and CST with small shift in the cut-off frequencies. Let us present in Fig. 6 the distribution electric field computed by the Matlab code using the mesh of Fig. 2 (b) and Fig. 4 (b). The electric field is present in these figure are plotted at different frequencies at 60 GHz, 65 GHz and 70 GHz. It can be observed that the electric field distribution of the  $TE_{10}$  fundamental modes is well

contained in the waveguide and an efficient repartition of the electric field is observed

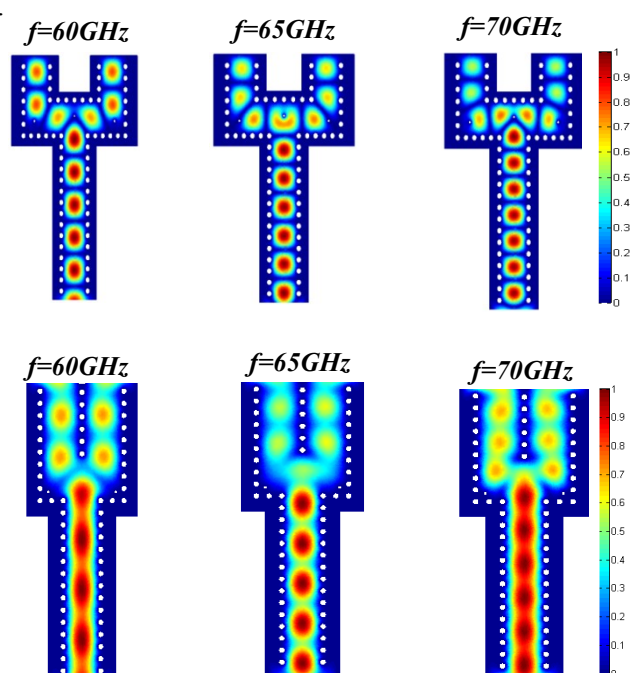


Fig. 6 The distribution electric fields of the T and Y-junction.

## 5 Conclusions

In this paper, an efficient FEM algorithm to analyze discontinuities in T and Y junction SIW power dividers has been presented. The applicability of the method has been illustrated in the SIW power dividers. Finally, it has been applied to analyze a T and Y-junction, the validity of the CST commercial software results is analyzed by showing field plots and comparison with the FEM tools is programmed with Matlab code. The FEM method is a powerful and simple tool for modelling these kinds of structures. These structures can be easily fabricated and conveniently be integrated into microwave and millimeter wave integrated circuits for mass production with low cost and small size.

### References:

- [1] Z.-C. Hao, W. Hong, J.-X. Chen, X.-P. Chen, and K. Wu, "Compact super-wide bandpass substrate integrated waveguide (SIW) filters," *IEEE Trans. Microw. Theory Techn.*, vol. 53, no. 9, pp. 2968–2977, Sep. 2005.
- [2] Y. D. Dong, T. Yang, and T. Itoh, "Substrate integrated waveguide loaded by complementary split-ring resonators and its applications to miniaturized waveguide filters,

" *IEEE Trans. Microw. Theory Techn.*, vol. 57, no. 9, pp. 2211–2223, Sep. 2009.

- [3] L. Yan, W. Hong, G. Hua, J. Chen, K. Wu, and T. J. Cui, "Simulation and experiment on SIW slot array antennas," *IEEE Microw. Wireless Compon. Lett.*, vol. 14, no. 9, pp. 446–448, Sep. 2004.
- [4] M. Henry, C. Free, B. Izqueirido, J. Batchelor, and P. Young, "Millimeter wave substrate integrated waveguide antennas: Design and fabrication analysis," *IEEE Trans. Adv. Packag.*, vol. 32, no. 1, pp. 93–100, Feb. 2009.
- [5] D. Deslandes and K. Wu, "Integrated microstrip and rectangular waveguide in planar form," *IEEE Microw. Wireless Compon. Lett.*, vol. 11, no. 2, pp. 68–70, Feb. 2001.
- [6] D. Deslandes and K. Wu, "Analysis and design of current probe transition from grounded coplanar to substrate integrated rectangular waveguides," *IEEE Trans. Microw. Theory Techn.*, vol. 53, no. 8, pp. 2487–2494, Aug. 2005.
- [7] E. Diaz, A. Belenguer, H. Esteban, O. Moneris-Belda, and V. Boria, "A novel transition from microstrip to a substrate integrated waveguide with higher characteristic impedance," in *IEEE MTT-S Int. Microw. Symp. Dig.*, 2013, pp. 1–4.
- [8] J.-X. Chen, W. Hong, Z.-C. Hao, H. Li, and K. Wu, "Development of a low cost microwave mixer using a broadband substrate integrated waveguide (SIW) coupler," *IEEE Microw. Wireless Compon. Lett.*, vol. 16, no. 2, pp. 84–86, Feb. 2006.
- [9] Y. Cassivi and K. Wu, "Low cost microwave oscillator using substrate integrated waveguide cavity," *IEEE Microw. Wireless Compon. Lett.*, vol. 13, no. 2, pp. 48–50, Feb. 2003.
- [10] G. Pelosi, R. Coccioli, S. Selleri, "Quick Finite Elements for Electromagnetic Waves," *Second Edition*, Boston: Artech House, 2009.
- [11] Germain. S, Deslandes.D, Wu Ke, "Development of substrate integrated waveguide power dividers," *Electrical and computer Engineering, 2003.IEEE CCECE 2003.Canadian Conference on*, vol.3,4-7 pp:1921-1924,May 2003
- [12] M. A. Rabah, M. Abri, J. Tao, and T. H. Vuong, "Substrate integrated waveguide design using the two dimentionnal finite element method", *PIER M*, Vol. 35, 21-30, 2014.
- [13] R. Shewchuk, "Delaunay refinement algorithms for triangular mesh generation". *Comput. Geom.* Vol. 47, No. 7, pp. 741-778, 2014.